ISSN: 1410-8917
e-ISSN: 2597-9914

Jurnal Kimia Sains dan Aplikasi 27 (10) (2024): 499-509

Jurnal Kimia Sains dan Aplikasi
Journal of Scientific and Applied Chemistry

Journal homepage: http://ejournal.undip.ac.id/index.php/ksa

Design, Fabrication, and Testing of Salt Spray as An Atmospheric Corrosion Test Tool Using $MgCl_2$ and NaCl Solutions

Sri Hastuty [1,*], Darius Tegar Oktaviyanto [1], Fatwa Khoirrun Nadhor [1], Wahyu Caesarendra [2], Muhammad Awwaluddin [3]

[1] Mechanical Engineering Department, Universitas Pertamina, Jl. Teuku Nyak Arief, RT.7/RW.8, Simprug, Kec. Kby. Lama, Kota Jakarta Selatan, Daerah Khusus Ibukota Jakarta 12220, Indonesia
[2] Faculty of Integrated Technology, Universiti Brunei Darussalam, Gadong BE1410, Brunei Darussalam
[3] Research Organization of Energy and Manufacturing, National Research and Innovation Agency, 15310 Serpong, Indonesia

* Corresponding author: sri.hastuty@universitaspertamina.ac.id

https://doi.org/10.14710/jksa.27.10.499-509

Article Info

Article history:

Received: 03rd April 2024
Revised: 27th August 2024
Accepted: 01st October 2024
Online: 30th October 2024

Keywords:
Atmospheric Corrosion; $MgCl_2$; NaCl; Salt Spray Chamber; Steel ST 37; SS 304

Abstract

The research aimed to design a salt spray chamber adhering to ASTM-B117 standards and test the chamber with determine the atmospheric corrosion rate in a salt spray chamber using steel materials (ST 37 and SS 304) in NaCl and $MgCl_2$ solutions. Corrosion tests spanned 48 hours, with time variables of 4, 6, and 8 hours of wet and dry cycle for 48 hours total. The objective was to design salt spray chamber and test the chamber to compare the corrosion rate based on solution and material selected. Visual inspections post-corrosion included macro photos, microscopy, SEM, and EDS analyses. Weight loss in Steel ST 37, cleaned per ASTM G1 with HCl, was also assessed. Corrosion rates of Steel ST 37 varied marginally across time variables and solutions. NaCl corrosion rates at 4, 6, and 8 hours averaged 4.5232, 5.8418, and 6.7148 mmpy, respectively. For $MgCl_2$, rates were 4.2564, 5.3436, and 6.0915 mmpy, respectively. Stainless steel exhibited higher resistance compared to Steel ST 37. In conclusion, both NaCl and $MgCl_2$ solutions accelerate corrosion, with NaCl inducing a higher rate. Stainless steel outperforms Steel ST 37, and the chamber material displays resilience against atmospheric corrosion.

1. Introduction

Corrosion, an inevitable natural phenomenon, poses significant challenges across various industries and in our daily lives. Its adverse effects on infrastructure, equipment, and materials are well-documented, leading to substantial economic losses and safety concerns [1]. Among the various forms of corrosion, atmospheric corrosion stands out as a pervasive and unavoidable threat, constantly degrading exposed materials [2]. Corrosion presents several significant disadvantages in industry, leading to considerable economic repercussions and operational challenges. Supported by extensive data, these drawbacks are pervasive and multifaceted. Financially, corrosion-related costs amount to approximately $2.5 trillion annually globally, representing a substantial portion of the global GDP. This expenditure encompasses maintenance, repair, and replacement of corroded equipment and infrastructure.

Furthermore, corrosion-induced downtime disrupts production schedules, resulting in decreased productivity and revenue loss, with the U.S. economy alone facing over $276 billion in annual losses attributed to corrosion-related downtime. Safety hazards abound as corrosion compromises the structural integrity of equipment and infrastructure, posing risks to both workers and the public. Environmental consequences are equally dire, with corrosion-related leaks and spills leading to soil and water contamination, habitat destruction, and adverse health effects on ecosystems and wildlife. Premature asset degradation due to corrosion necessitates increased capital expenditures and lifecycle costs for industries, with up to 25% of annual corrosion costs deemed avoidable through effective corrosion prevention and mitigation strategies [3, 4, 5].

Atmospheric corrosion, an inevitable consequence of exposure to environmental elements, poses significant

challenges across various industries and infrastructural domains [2]. It occurs when materials are subjected to atmospheric conditions containing moisture, oxygen, pollutants, and other corrosive agents [2]. Unlike localized forms of corrosion that can be mitigated through protective coatings or design modifications, atmospheric corrosion affects exposed surfaces uniformly, gradually deteriorating materials over time. Its pervasive nature makes it a concern for structures, equipment, and materials in diverse environments, including coastal regions, industrial areas, and urban settings. Atmospheric corrosion not only compromises the integrity and performance of metal structures but also impacts safety, aesthetics, and economic viability. Consequently, understanding the mechanisms and factors influencing atmospheric corrosion is crucial for implementing effective mitigation strategies and ensuring the durability and longevity of assets in the face of environmental challenges [6, 7, 8].

To combat the detrimental effects of atmospheric corrosion, reliable testing methods are imperative for assessing material performance and durability. One widely used approach is the utilization of salt spray chambers [9], which simulate harsh environmental conditions to accelerate corrosion processes and evaluate material susceptibility. A salt spray chamber, also known as a salt fog chamber or salt spray test chamber, replicates the corrosive conditions encountered in marine and coastal environments [10]. It creates a controlled atmosphere of salt-laden mist, accelerating corrosion reactions and facilitating accelerated testing of materials [11, 12]. The suitability of salt spray chambers for atmospheric corrosion testing stems from their ability to simulate corrosive conditions in a controlled and reproducible manner, allowing for comparative evaluations of material performance.

This study focuses on two commonly used materials in industrial applications: Steel ST 37 and SS 304. Steel ST 37, classified as structural steel, is endowed with several physical properties that render it conducive for a plethora of industrial applications. Notably, its density typically ranges between 7.85 and 7.87 g/cm^3, imparting a balance between structural strength and lightweight characteristics. Furthermore, Steel ST 37 exhibits a tensile strength typically spanning from 360 to 510 MPa, alongside a yield strength of approximately 235 MPa. These mechanical properties signify its capacity to endure applied loads without succumbing to plastic deformation.

Moreover, Steel ST 37 showcases remarkable ductility, often boasting an elongation percentage exceeding 20%, thus allowing it to deform substantially before fracture under tensile stress. In terms of hardness, this steel typically registers between 170 to 210 HB (Brinell hardness), signifying notable resistance to indentation and abrasion. With a melting point typically ranging from 1,370°C to 1,480°C, Steel ST 37 remains steadfast even under elevated temperatures, ensuring its reliability in applications exposed to heat. Additionally, being ferromagnetic, Steel ST 37 can be magnetized, presenting advantageous magnetic properties suitable for diverse applications such as electromagnetic devices and magnetic sensors [13, 14, 15, 16]. These physical attributes collectively underscore the versatility and efficacy of Steel ST 37 across various domains, encompassing construction, manufacturing, automotive engineering, and machinery production. It is essential to recognize that these properties may slightly vary contingent upon manufacturing processes, alloy compositions, and specific material standards. However, its susceptibility to corrosion, particularly in corrosive environments, necessitates comprehensive evaluation.

Stainless Steel 304 (SS 304), an austenitic stainless steel alloy, is renowned for its exceptional corrosion resistance and versatility. Composed primarily of iron, chromium, and nickel, SS 304 exhibits superior resistance to oxidation, corrosion, and staining, making it ideal for applications requiring durability and aesthetic appeal. SS 304, a widely utilized alloy renowned for its corrosion resistance and versatility, boasts a myriad of physical properties that render it indispensable in both daily life and industrial applications. With its exceptional resistance to oxidation, corrosion, and staining, SS 304 is a preferred choice across various sectors, including construction, automotive, food processing, and pharmaceuticals. Its density typically ranges between 7.93 and 8.0 g/cm^3, providing a robust yet lightweight material for structural and aesthetic purposes. Moreover, SS 304 exhibits impressive tensile strength, usually between 515 and 690 MPa, coupled with a yield strength of approximately 205 MPa, ensuring durability under diverse loading conditions [17, 18, 19, 20, 21]. Commonly utilized in architectural, food processing, and pharmaceutical industries, SS 304 offers unparalleled longevity and performance in corrosive environments.

To simulate realistic corrosive environments, we conducted corrosion tests using NaCl and $MgCl_2$ solutions, representing common salts found in coastal and industrial atmospheres. Both salts are known contributors to atmospheric corrosion, exacerbating material degradation and necessitating comprehensive evaluation. The primary objective of this study is to design and evaluate the performance of a salt spray chamber for atmospheric corrosion testing. Our focus lies in designing a chamber capable of replicating corrosive atmospheric conditions accurately. Subsequently, we aim to assess the corrosion resistance of Steel ST 37 and SS 304 under simulated environments within the designed chamber. This evaluation will provide valuable insights into the comparative performance of these materials in the face of atmospheric corrosion.

Furthermore, we intend to investigate the effectiveness of NaCl and $MgCl_2$ solutions in accelerating atmospheric corrosion processes [22, 23]. By subjecting the materials to these solutions, we seek to simulate realistic corrosive environments encountered in coastal and industrial settings. Finally, our study aims to evaluate the performance and reliability of the designed salt spray chamber. Through comprehensive testing and analysis, we aim to ascertain the chamber's suitability for future corrosion studies and its potential contribution to

advancing our understanding of material degradation mechanisms.

2. Experimental

This research focused on the design and fabrication of a salt spray chamber, followed by performance testing to investigate the corrosion behavior of two commonly used materials: Carbon Steel ST37 and SS 304. The materials were exposed to simulated atmospheric conditions using solutions of 3.5 wt% NaCl and 3.5 wt% $MgCl_2$. Prior to corrosion testing, the surface of the specimens was examined using macroscopic, microscopic, and SEM analysis. After the corrosion testing, the surfaces were again observed using macroscopic, microscopic, SEM, and EDS techniques to identify the morphology and corrosion products.

2.1. Design of Salt Spray Chamber

The salt spray chamber was designed according to ASTM B 117 standards. The design was utilized the SolidWorks application. The salt spray chamber was constructed from acrylic, as seen in Figure 1. Figure 2 shows the dimensions of the salt spray chamber. The chamber cover was made slanted so that adhering mist deposits would not drip on the surface of the specimen, the mist maker was placed in the side chamber, the sample was placed in the middle of the chamber , and a small hole for the mist generator cable. The salt spray chamber was then tested for leaks, which carried out by filling the solution holding chamber with 3 L of water and then letting it sit for 1 hour to ensure that the chamber that has been installed did not experience leaks. The chamber shows no leak during this test.

Figure 1. Salt spray chamber

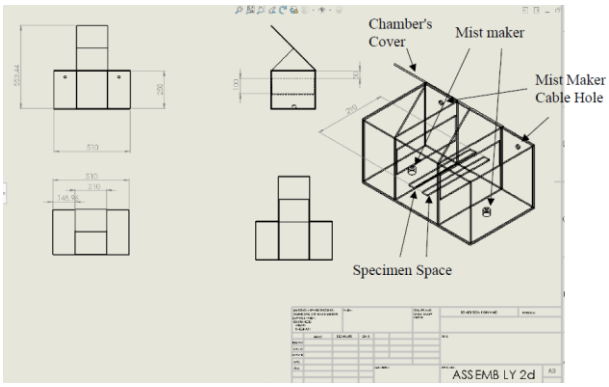

Figure 2. Dimension of salt spray chamber

2.2. Materials

Carbon Steel ST 37 and SS 304 were meticulously prepared as specimens, with the former cut to dimensions of 200 × 200 × 3 mm and the latter to 200 × 200 × 2 mm. The surfaces were ground using 400, 800, and 1000 grit sandpaper to achieve a smooth finish. Solutions of 3.5 wt% NaCl and 3.5 wt% $MgCl_2$ were prepared, each with a volume of 10 liters. These dimensions and preparations were selected to ensure representative samples for testing in the salt spray chamber.

2.3. Corrosion Testing

The corrosion testing incorporated a mist maker into the chamber set up to facilitate the creation of controlled atmospheric conditions using a solution consisting of 3.5 wt% NaCl and 3.5 wt% $MgCl_2$. Before testing, the initial weights of each the specimens were recorded to establish a baseline for corrosion assessment.

The specimens underwent a rigid corrosion testing process following meticulous preparation, exposing them to the salt spray chamber for 48 hours. The testing included variable misting and drying intervals of 4, 6, and 8 hours to simulate diverse environmental conditions. Figure 3 shows the corrosion testing process. During the testing periode, the relative humidity and temperature were also monitored using datalog. After the testing period, the specimens were carefully cleaned using 1 M of HCl solution at room temperature to remove any corrosion products, enabling accurate weight loss measurement. Subsequent reweighing of the specimens facilitated the calculation of corrosion rates utilizing the weight loss method according to Equation 1. This comprehensive approach, combined with multiple experimental replicates, ensured the reliability and reproducibility of the findings, thus contributing to the advancement of corrosion science and materials engineering.

$$Corrosion\ Rate\ (mmpy) = \frac{K \times W}{D \times A \times T} \quad (1)$$

Where K is the constant value of is a constant with value 8.76×10^8, W is the difference in load (grams), A is the surface area (cm^2), T is the immersion time (hours), and D is the density (g/cm^3).

Figure 3. Atmospheric corrosion testing

3. Results and Discussion

This research investigated the corrosion behavior under simulated atmospheric conditions and examined the morphology of the samples using macroscopic, microscopic, and SEM-EDS analysis.

3.1. Morphology Before Corrosion Testing

Before corrosion testing was employed, the surface of the Steel ST 37 and SS 304 was observed using macroscopic, microscopic, and SEM analysis. Figure 4 shows the surface of the material before testing.

3.2. Corrosion Testing of Steel ST 37 with Salt Spray of 3.5 wt% NaCl

The corrosion testing utilizing 3.5 wt% NaCl was conducted, and the surface of steel ST 37 was observed from macroscopic, microscopic, and SEM. Figure 5 is a macro photo of the sample after corrosion testing. On the Steel ST37 plate, corrosion occurs, covering the entire surface of the specimen after the corrosion process is carried out. For the 8-hour variable, the corrosion products that occur on the surface of the specimen are more visible and evenly distributed compared to 4 and 6 hours.

Figure 6 is a microscope photo with a magnification of 50×; it can be seen that corrosion products occur mostly in variables 8 and 6, whereas at 4 hours, the corrosion that occurs is not as much as 6 and 8 hours. An increase in corrosion products can be seen as the variable test time used increases. Figure 6 shows that in the 6 and 8-hour tests, there was a buildup of corrosion products on the sample surface, indicated by a textured microscopic image. Meanwhile, in the 4-hour test, there was no accumulation of corrosion products as severe as in the 6 and 8-hour tests.

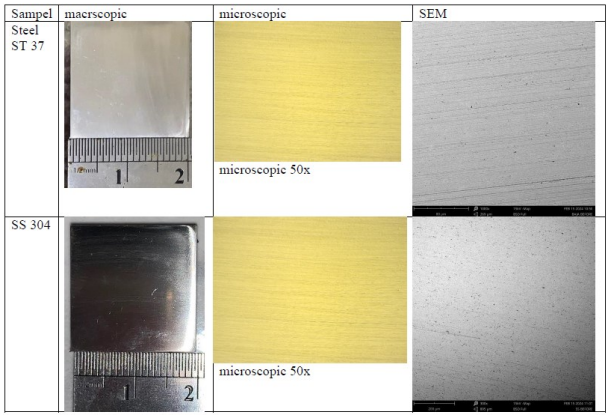

Figure 4. Surface before corrosion testing

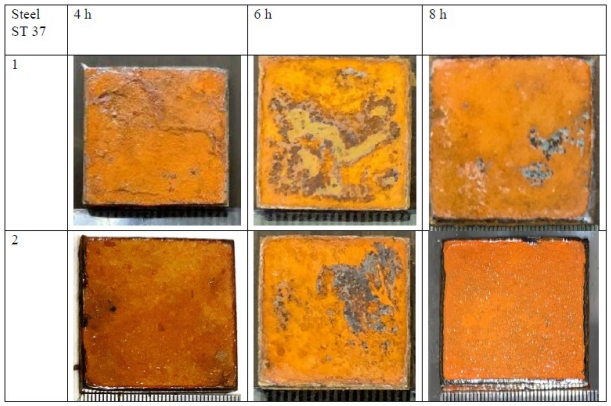

Figure 5. Macroscopic of Steel ST 37 after testing with 3.5 wt% NaCl

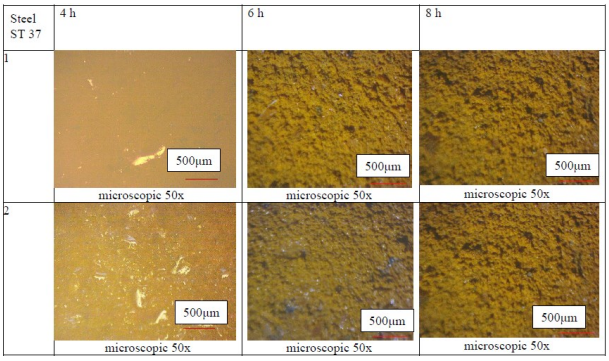

Figure 6. Microscopic of Steel ST 37 after testing with 3.5 wt% NaCl

Figure 7 shows the results of SEM observations on steel for 4-hour and 6-hour intervals, with magnifications of 1000× and 1500×. In the 4-hour interval, the corrosion appears in larger grains, whereas in the 6-hour interval, the corrosion takes the form of smaller, finer grains. Figure 8 illustrates the element mapping of the corroded surface of Steel ST37 tested with 3.5 wt% NaCl for 4 hours. Figure 9 displays the distribution of Fe, O, and Cl elements on the corroded surface. The Fe element is the most dominant and is evenly distributed across the surface. Table 1 shows the concentration of each element, indicating that Fe is the dominant element, followed by O with a weight concentration of 22.48%, and a small amount of Cl with a concentration of 5.26%.

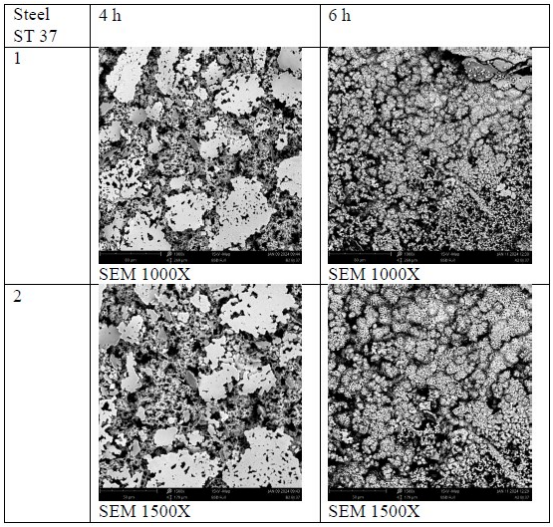

Figure 7. SEM images of Steel ST 37 after testing with 3.5 wt% NaCl

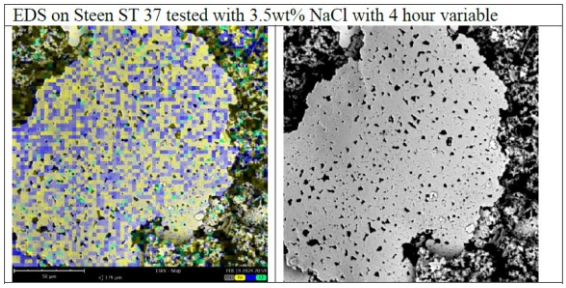

Figure 8. EDS images of Steel ST 37 after testing with 3.5 wt% NaCl for 4 hours interval

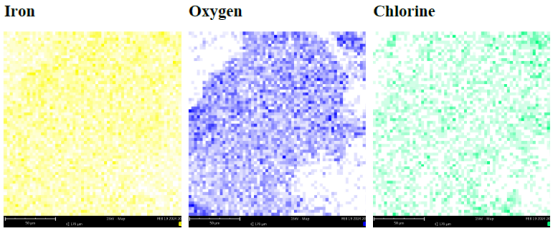

Figure 9. Element distribution of Steel ST 37 after testing with 3.5 wt% NaCl for 4 hours

Table 1. Element composition of Steel ST 37 after testing with 3.5 wt% NaCl for 4 hours interval

Element number	Element symbol	Element name	Atomic conc.	Weight conc.
26	Fe	Iron	45.44	72.26
8	O	Oxygen	49.35	22.48
17	Cl	Chlorine	5.21	5.26

Figure 10 shows the SEM-EDS results after 8 hours of exposure to NaCl, it indicates that the form of corrosion is like tiny fibres covering the surface with slight island-like shapes, and the distribution of iron and oxygen is still accumulating in several areas. Figure 11 illustrates the distribution of Fe, O, and Cl elements. Fe is distributed evenly across the surface, while O and Cl are localized in specific areas. Table 2 presents the concentration of each element by weight, showing that Fe is the most dominant element on the surface, followed by O and Cl. The presence of O and Cl suggests the formation of corrosion products on the surface.

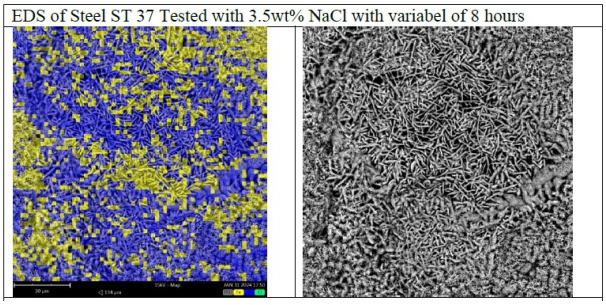

Figure 10. EDS images of Steel ST 37 after testing with 3.5 wt% NaCl for 8 hours

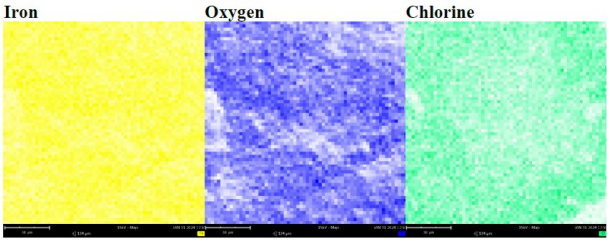

Figure 11. Element distribution of Steel ST 37 after testing with 3.5wt % NaCl for 8 hours

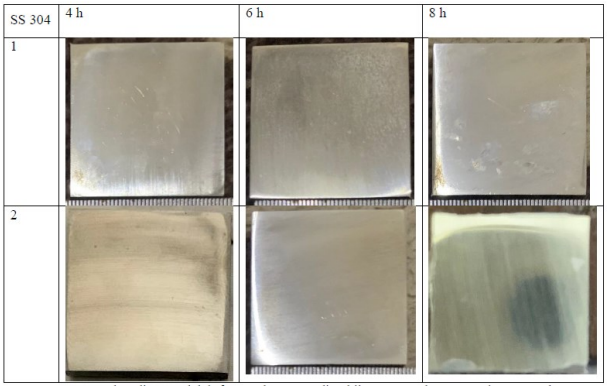

Figure 12. Macroscopic view of SS 304 after testing with 3.5 wt% NaCl

Table 2. Element composition of Steel ST 37 after testing with 3.5 wt% NaCl for 8 hours

Element number	Element symbol	Element name	Atomic conc.	Weight conc.
26	Fe	Iron	30.83	58.81
8	O	Oxygen	64.08	35.02
17	Cl	Chlorine	5.09	6.17

3.3. Corrosion Testing of SS 304 with 3.5 wt% NaCl

Figure 12 shows the macroscopic view of the surface of SS 304. No changes in either color or shape are observed, indicating that no corrosion occurred on the surface of SS 304. Figure 13 shows the microscopic view of the surface of SS 304 at a magnification of 50×. No corrosion products are observed on the surface. SS 304 exhibits high resistance to atmospheric corrosion due to its composition, which includes chromium and nickel. These elements form a passive layer on the surface, protecting it from corrosion. Furthermore, the material's low solubility in water reduces the likelihood of corrosion [24]. Figure 14 presents the SEM observation of the surface, revealing only some salt deposits.

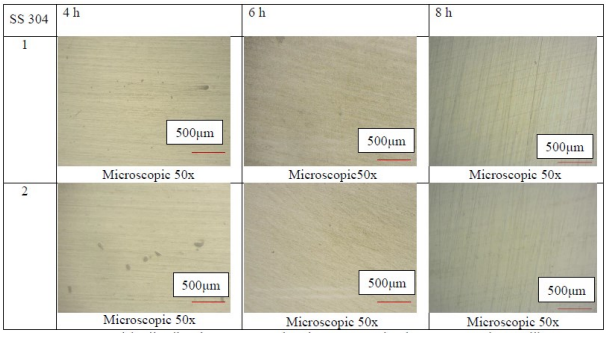

Figure 13. Microscopic view of SS 304 after testing with 3.5 wt% NaCl

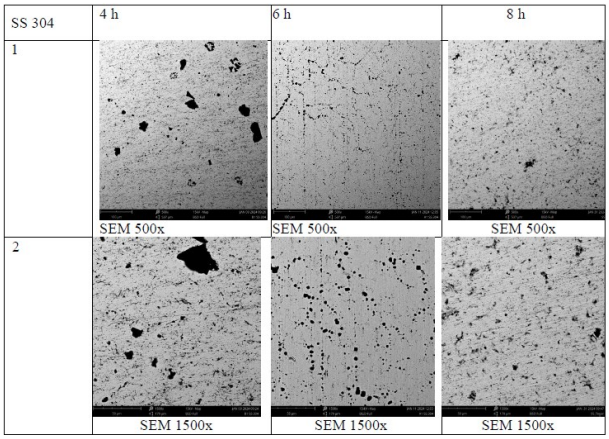

Figure 14. SEM images of SS 304 after testing with 3.5 wt% NaCl

3.4. Corrosion Testing of Steel ST 37 with Salt Spray of 3.5 wt% $MgCl_2$

Figure 15 shows a macro photograph of the Steel ST 37 plate, where corrosion is observed, covering the entire surface of the specimen after the corrosion process. For the 8-hour variable, the corrosion products on the surface are more numerous and evenly distributed compared to the 4-hour and 6-hour variables. Corrosion at 4 hours is less pronounced than at 6 and 8 hours. This suggests a change in color to orange, indicating the presence of corrosion.

Figure 16 presents a microscopic image at 50× magnification. The buildup of corrosion is most significant in the 6-hour and 8-hour variables, while at 4 hours, corrosion is noticeably less. The increase in corrosion products corresponds to the longer test durations. Figure 17 displays the SEM analysis of an Steel ST 37 plate corroded using a $MgCl_2$ solution. The SEM results for the 4-hour variable reveal corrosion in the form of small islands evenly distributed on the surface. At 6 hours, the corrosion appears as larger island-like formations.

Figure 18 displays the element mapping of Steel ST 37 corroded with 3.5 wt% MgCl2 for 4 hours, while Figure 19 shows the Fe, O, and Cl distributions. Fe is dominant and evenly distributed, as detailed in Table 3, which lists Fe as the most abundant element, followed by O at 13.56% and Cl at 0.73% by weight.

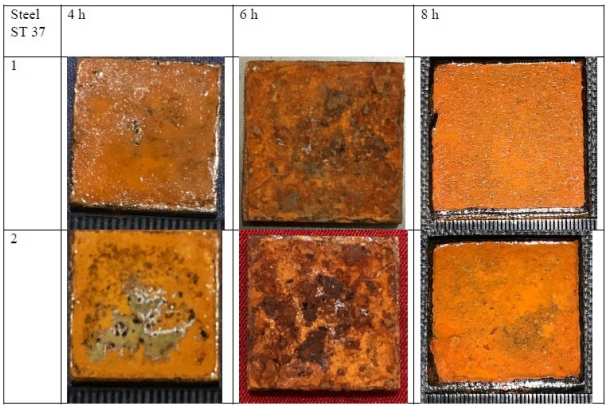

Figure 15. Macroscopic view of Steel ST 37 after testing with 3.5 wt% $MgCl_2$

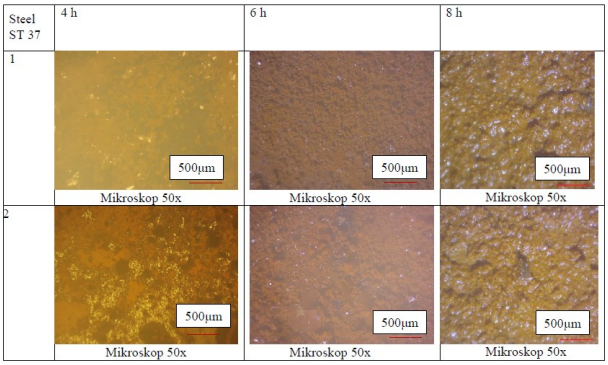

Figure 16. Microscopic view of Steel ST37 after testing with 3.5 wt% $MgCl_2$

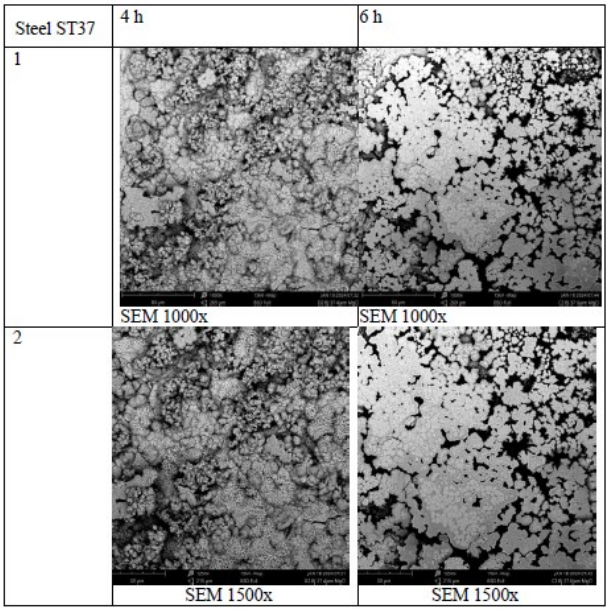

Figure 17. SEM images of Steel ST37 after testing with 3.5 wt% $MgCl_2$

Table 3. Element composition of Steel ST 37 after testing with 3.5 wt% $MgCl_2$ for 4 hours

Element number	Element symbol	Element name	Atomic Conc.	Weight Conc.
26	Fe	Iron	63.86	85.7
8	O	Oxygen	35.28	13.56
17	Cl	Chlorine	0.86	0.73

Figure 20 shows the SEM-EDS results for 8 hours of exposure to $MgCl_2$, revealing that the corrosion appears as tiny fibers covering the surface, with slight island-like formations. The distribution of Fe and O is still concentrated in several areas. Figure 21 illustrates the distribution of Fe, O, and Cl elements. Fe is distributed evenly across the surface, while O and Cl are localized in certain areas. Table 4 presents the weight concentrations of each element, indicating that Fe is the most dominant on the surface, followed by O and Cl. The presence of O and Cl suggests the formation of corrosion products on the surface.

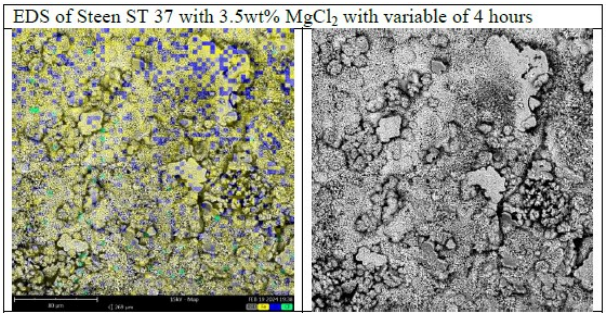

Figure 18. EDS images of Steel ST 37 after testing with 3.5 wt% $MgCl_2$ for 4 hours

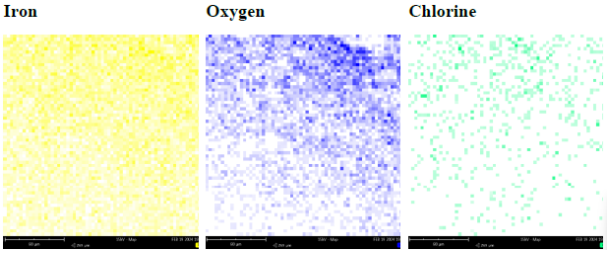

Figure 19. Element distribution of Steel ST 37 after testing with 3.5 wt% $MgCl_2$ for 4 hours

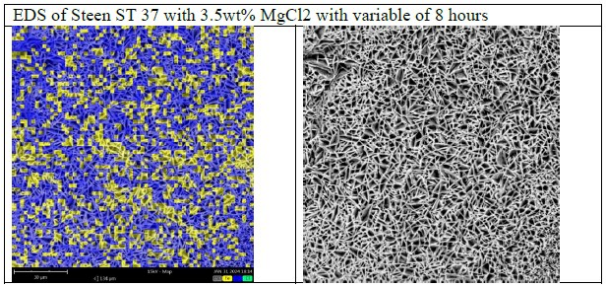

Figure 20. EDS images of Steel ST 37 after testing with 3.5 wt% $MgCl_2$ for 8 hours

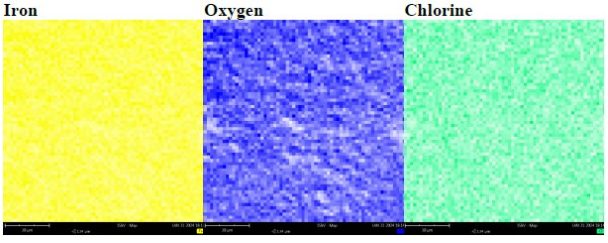

Figure 21. Element distribution of Steel ST 37 after testing with 3.5 wt% $MgCl_2$ for 8 hours

3.5. Corrosion Testing of SS 304 with Salt Spray of 3.5 wt% $MgCl_2$

Figure 22 shows the macroscopic view of SS 304 after exposure to the $MgCl_2$ solution. No visible corrosion is observed on the surface at any of the test time intervals. Figure 23 presents the microscopic results, where no visible corrosion is seen on the surface of the SS 304 sample for any of the test time intervals. Figure 24 shows the SEM results, revealing only salt deposits on the surface of SS 304, indicating that corrosion on the sample surface has not yet occurred.

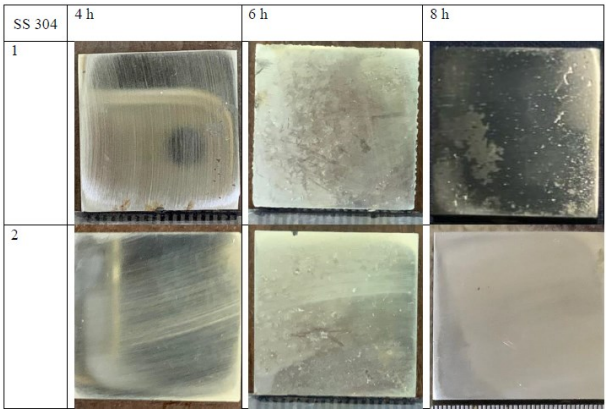

Figure 22. Macroscopic view of SS 304 after testing with 3.5 wt% $MgCl_2$

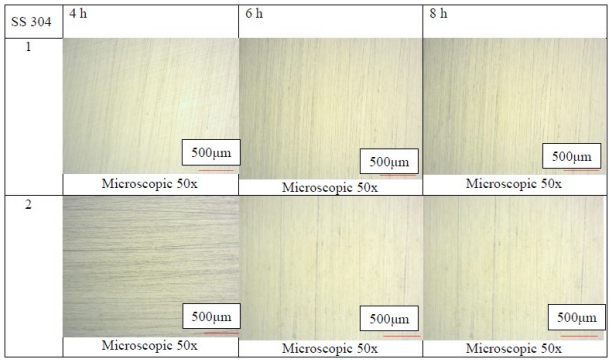

Figure 23. Microscopic view of SS 304 after testing with 3.5 wt% $MgCl_2$

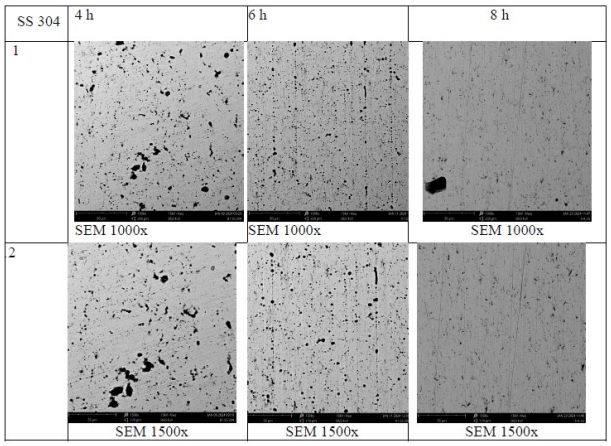

Figure 24. SEM images of SS 304 after testing with 3.5 wt% $MgCl_2$

3.6. Corrosion Rate

Following the conclusion of the corrosion testing procedure using salt spray, the specimen was cleaned with a 1 M HCl solution, in accordance with the stipulations outlined in ASTM G11 standards. However, since corrosion was only observed on Steel ST 37, the corrosion rate was calculated exclusively for this steel type, as no corrosion products were detected on the SS 304 samples. Figures 25 and 26 show the samples after cleaning, indicating that no corrosion products remain on the surface. After the cleaning process with HCl, the specimens were weighed, and the corrosion rate was determined, as detailed in Tables 5 and 6.

Figure 27 depicts a graphical representation illustrating the average corrosion rate over time. It is evident from the graph that with increasing hour intervals, there is a corresponding escalation in the corrosion rate. Furthermore, experimentation utilizing NaCl exhibits a significantly higher corrosion rate compared to tests conducted with $MgCl_2$.

The increase in corrosion rate correlates with the higher concentrations of O and Cl elements on the corroded surface (Figure 28). The higher corrosion rate, accompanied by increased O and Cl content on the corroded surface of steel, can be explained by the interaction of these elements with the steel. Both O and Cl promote corrosion in various materials, including steel. Oxygen can react with the steel surface to form oxides, acting as a catalyst for further corrosion [25].

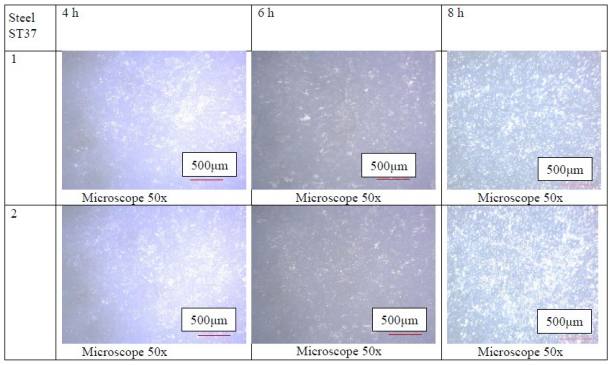

Figure 25. Microscopic view of Steel ST 37 with 3.5 wt% NaCl after cleaning with 1 M HCl

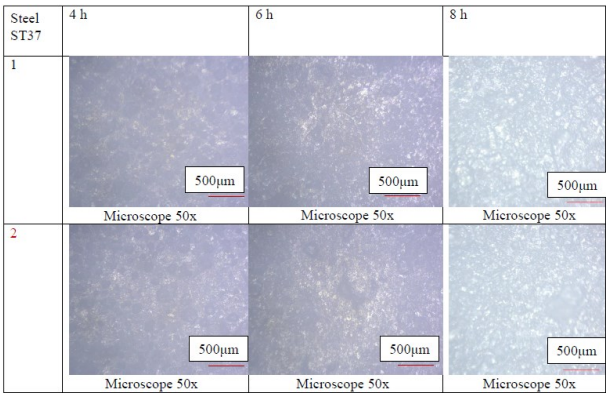

Figure 26. Microscopic view of Steel ST 37 with 3.5 wt% $MgCl_2$ and cleaning with 1 M HCl

Table 4. Element composition of Steel ST 37 after testing with 3.5 wt% $MgCl_2$ for 8 hours

Element number	Element symbol	Element name	Atomic conc.	Weight conc.
26	Fe	Iron	31.41	59.66
8	O	Oxygen	64.01	34.82
17	Cl	Chlorine	4.58	5.52

Table 5. Weight loss and corrosion rate of Steel ST 37 in 3.5 wt% NaCl

Sample	Initial weight (gr)	Final weight (gr)	Weight loss (gr)	Density (g/cm^3)	Corrosion rate (mm/y)
4-hour NaCl					
1	9.3814	9.1831	0.1983	7.86	4.4272
2	8.586	8.3764	0.2096	7.86	4.6794
3	9.1439	8.9413	0.2026	7.86	4.5232
Average (mmpy)					4.5433
6-hour NaCl					
1	9.0388	8.779	0.2598	7.86	5.8002
2	9.0057	8.745	0.2607	7.86	5.8203
3	9.3413	9.0768	0.2645	7.86	5.9051
Average (mm/y)					5.8418
8-hour NaCl					
1	9.5206	9.2175	0.3031	7.86	6.7669
2	9.3374	9.0393	0.2981	7.86	6.6553
3	9.215	8.9139	0.3011	7.86	6.7222
Average (mm/y)					6.7148

Table 6. Weight loss and corrosion rate of Steel ST 37 in 3.5 wt% $MgCl_2$

Sample	Initial weight (gr)	Final weight (gr)	Weight loss (gr)	Density (gr/cm^3)	Corrosion rate (mm/y)
4-hour $MgCl_2$					
1	9.3492	9.1558	0.1934	7.86	4.3178
2	9.2246	9.0367	0.1879	7.86	4.195
Average					4.2564
6-hour $MgCl_2$					
1	7.7639	7.5238	0.2401	7.86	5.3604
2	9.1293	8.8907	0.2386	7.86	5.3169
Average					5.3436
8-hour $MgCl_2$					
1	9.2391	8.9779	0.2612	7.86	5.8314
2	9.1645	8.88	0.2845	7.86	6.3516
Average					6.0915

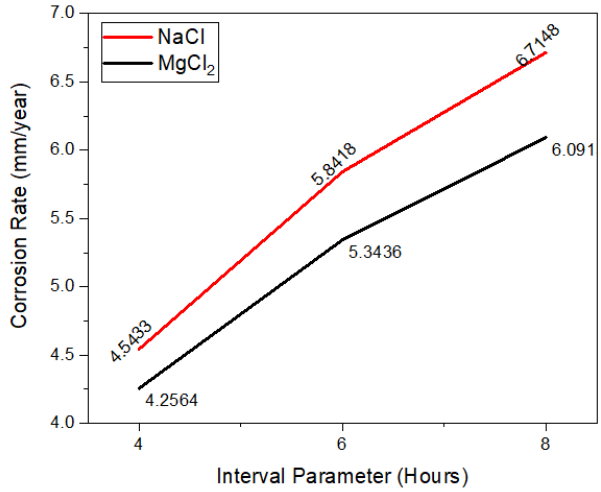

Figure 27. Corrosion rate of Steel ST 37

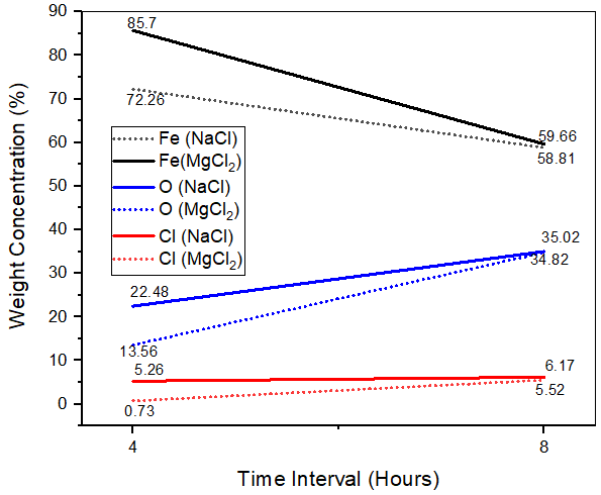

Figure 28. The weight concentration of Fe, O, and Cl ions after corrosion testing

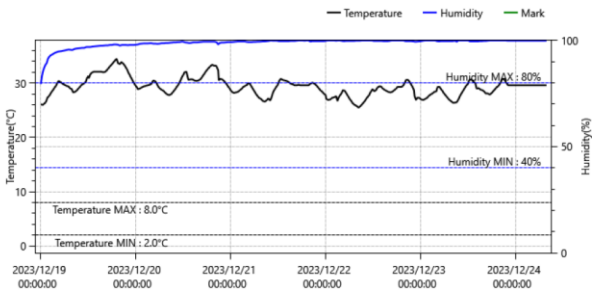

Figure 29. Temperature and relative humidity

In the case of high-strength steel, the EDS analysis shows an increase in FeO content, a steel oxide, with increasing immersion time, indicating that the steel is undergoing oxidation, leading to a higher corrosion rate [26]. Conversely, chlorine can form chlorides with the steel, which may dissolve into the surrounding environment. This can lead to the loss of the corrosion product and an increase in the corrosion rate. For low-alloy marine steel, it has been reported that the corrosion rate increases with the available chlorine concentration in seawater [27]. In summary, the higher corrosion rate, with increased O and Cl content on the corroded surface of steel, results from the interaction of these elements with the steel, leading to the formation of oxides and chlorides, which promote further corrosion.

The higher corrosion rate of steel in NaCl compared to $MgCl_2$ can be attributed to several factors. Firstly, the galvanic corrosion effect is more pronounced in NaCl, where the steel acts as the anode and NaCl as the cathode, resulting in a higher corrosion rate due to the increased flow of electrons from the anode to the cathode [28]. Secondly, the corrosion products formed on the steel surface in NaCl are generally more soluble than those formed in $MgCl_2$. This increased solubility leads to a higher dissolution rate of the corrosion products, thus accelerating the corrosion rate of the steel [29]. Furthermore, the presence of chloride ions in NaCl promotes the formation of more soluble corrosion products, further increasing the corrosion rate. Additionally, the formation of loose oxide layers on the steel surface in NaCl can result in a higher corrosion rate compared to $MgCl_2$, as these oxide layers are more easily dissolved or removed, exposing the underlying metal to further corrosion [30].

The higher content of O and Cl from NaCl on the corroded surface compared to $MgCl_2$ is likely due to NaCl being a stronger corrosive agent, which promotes the formation of more soluble corrosion products. As a result, higher concentrations of O and Cl ions are present on the steel's corroded surface exposed to NaCl than to $MgCl_2$ [30]. Figure 29 shows the temperature and relative humidity inside the salt spray chamber. The relative humidity ranged from 80% to 100%, while the temperature inside the chamber fluctuated between 28°C and 34°C. Figure 29 also illustrates the temperature and relative humidity during the testing period, showing a relative humidity range of 80% to 100%, with temperatures fluctuating between 26°C and 34°C.

4. Conclusion

In conclusion, the salt spray chamber design, adhering to ASTM B117 standards, effectively facilitates corrosion testing. Key features include a mist test chamber, angled cover, mist generator, and solution collection area, maintaining conditions of 35°C±2°C and 95%±5% humidity. A 336-hour salt spray test validated its performance, demonstrating effective mist deposition to simulate atmospheric corrosion despite the absence of a temperature controller. This design enables accurate corrosion rate characterization, proving its value in research and experimentation. The corrosion rates observed on Steel ST 37 and SS 304 differ notably, as evidenced by the absence of corrosion on SS 304 despite exposure to the same testing conditions that caused corrosion on ST 37 in a salt spray chamber. Further analysis reveals distinct corrosion rates between the two types of solutions used: NaCl and $MgCl_2$. Notably, for ST 37, corrosion rates with NaCl solution vary, averaging 4.232 mmpy at 4 hours, 5.8418 mmpy at 6 hours, and 6.7148 mmpy at 8 hours. Conversely, with $MgCl_2$ solution, corrosion rates average 4.2564 mmpy at 4 hours, 5.3436 mmpy at 6 hours, and 6.0915 mmpy at 8 hours. It can be inferred that the corrosion rates induced by both solutions are higher compared to NaCl alone.

References

[1] Pietro Pedeferri, Marco Ormellese, *Corrosion science and engineering*, Springer, 2018,

[2] Vladimir Kucera, Einar Mattsson, Atmospheric corrosion, in: *Corrosion Mechanisms*, CRC Press, 2020,

[3] A. A. El-Meligi, Corrosion preventive strategies as a crucial need for decreasing environmental pollution and saving economics, *Recent Patents on Corrosion Science*, 2, 1, (2010), 22-33 http://dx.doi.org/10.2174/1877610801002010022

[4] Gerhardus Koch, 1 - Cost of corrosion, in: A.M. El-Sherik (Ed.) *Trends in Oil and Gas Corrosion Research and Technologies*, Woodhead Publishing, Boston, 2017, https://doi.org/10.1016/B978-0-08-101105-8.00001-2

[5] Dariusz Kowalski, Beata Grzyl, Adam Kristowski, The Cost Analysis of Corrosion Protection Solutions for Steel Components in Terms of the Object Life Cycle Cost, *Civil and Environmental Engineering Reports*, 26, 3, (2017), 5-13 https://doi.org/10.1515/ceer-2017-0031

[6] Yikun Cai, Yuanming Xu, Yu Zhao, Xiaobing Ma, Atmospheric corrosion prediction: a review, *Corrosion Reviews*, 38, 4, (2020), 299-321 https://doi.org/10.1515/corrrev-2019-0100

[7] Yikun Cai, Yu Zhao, Xiaobing Ma, Kun Zhou, Yuan Chen, Influence of environmental factors on atmospheric corrosion in dynamic environment, *Corrosion Science*, 137, (2018), 163-175 https://doi.org/10.1016/j.corsci.2018.03.042

[8] Yuanjie Zhi, Zhihui Jin, Lin Lu, Tao Yang, Deyun Zhou, Zibo Pei, Dequan Wu, Dongmei Fu, Dawei Zhang, Xiaogang Li, Improving atmospheric corrosion prediction through key environmental factor identification by random forest-based model, *Corrosion Science*, 178, (2021), 109084 https://doi.org/10.1016/j.corsci.2020.109084

[9] Lietai Yang, *Techniques for Corrosion Monitoring*, 2nd ed., Woodhead Publishing, 2020, ^https://doi.org/10.1016/C2018-0-01137-8

[10] G. Wang, X. Tuo, L. Kou, W. Zhao, X. Zhu, Research on corrosion performance of 6061 aluminum alloy in salt spray environment, *Materialwissenschaft und Werkstofftechnik*, 51, 12, (2020), 1686-1699 https://doi.org/10.1002/mawe.202000081

[11] Minoru Ito, Azusa Ooi, Eiji Tada, Atsushi Nishikata, In Situ Evaluation of Carbon Steel Corrosion under Salt Spray Test by Electrochemical Impedance Spectroscopy, *Journal of The Electrochemical Society*, 167, 10, (2020), 101508 https://doi.org/10.1149/1945-7111/ab9c85

[12] B. J. Usman, F. Scenini, M. Curioni, Corrosion Testing of Anodized Aerospace Alloys: Comparison Between Immersion and Salt Spray Testing using Electrochemical Impedance Spectroscopy, *Journal of The Electrochemical Society*, 167, 4, (2020), 041505 https://doi.org/10.1149/1945-7111/ab74e3

[13] Mohammad Bahirai, Mohsen Gerami, Vahid Bahaari Zargar, Postannealing Mechanical Properties of Structural Steel St37, *Journal of Materials in Civil Engineering*, 32, 7, (2020), 04020152 https://doi.org/10.1061/(ASCE)MT.1943-5533.0003191

[14] Mostafa Jafarzadegan, Majid Ahangaryan, Reza Taghiabadi, Heat Input Effect on Microstructure and Mechanical Properties in Shielded Metal Arc Welding of Dissimilar AISI 316L/St-37 Steel, *International Journal of Iron & Steel Society of Iran*, 17, 1, (2021), 1-10

[15] Maryam Soleimani, Hamed Mirzadeh, Changiz Dehghanian, Phase transformation mechanism and kinetics during step quenching of st37 low carbon steel, *Materials Research Express*, 6, 11, (2019), 1165f1162 https://doi.org/10.1088/2053-1591/ab4960

[16] Rilis Eka Perkasa, Leonardo Gunawan, Sigit Puji Santosa, Afdhal Afdhal, Mechanical Anisotropy of Cold-Rolled St-37 Steel Plate Under High Strain Rates Loadings, *International Journal of Mechanical Engineering Technologies Applications*, 4, 2, (2023), 198-211 https://doi.org/10.21776/MECHTA.2023.004.02.9

[17] Weibo Huang, Yimin Zhang, Weibing Dai, Risheng Long, Mechanical properties of 304 austenite stainless steel manufactured by laser metal deposition, *Materials Science and Engineering: A*, 758, (2019), 60-70 https://doi.org/10.1016/j.msea.2019.04.108

[18] Meysam Naghizadeh, Hamed Mirzadeh, Effects of Grain Size on Mechanical Properties and Work-Hardening Behavior of AISI 304 Austenitic Stainless Steel, *steel research international*, 90, 10, (2019), 1900153 https://doi.org/10.1002/srin.201900153

[19] Francisco-Javier Cárcel-Carrasco, Manuel Pascual-Guillamón, Lorenzo Solano García, Fidel Salas Vicente, Miguel-Angel Pérez-Puig, Pitting Corrosion in AISI 304 Rolled Stainless Steel Welding at Different Deformation Levels, *Applied Sciences*, 9, 16, (2019), 3265 https://doi.org/10.3390/app9163265

[20] Amresh Kumar, Rajesh Sharma, Santosh Kumar, Prajjawal Verma, A review on machining performance of AISI 304 steel, *Materials Today: Proceedings*, 56, (2022), 2945-2951 https://doi.org/10.1016/j.matpr.2021.11.003

[21] Guosheng Sun, Linxiu Du, Jun Hu, Bin Zhang, R. D. K. Misra, On the influence of deformation mechanism during cold and warm rolling on annealing behavior of a 304 stainless steel, *Materials Science and Engineering: A*, 746, (2019), 341-355 https://doi.org/10.1016/j.msea.2019.01.020

[22] C. Örnek, D.L. Engelberg, Toward Understanding the Effects of Strain and Chloride Deposition Density on Atmospheric Chloride-Induced Stress Corrosion Cracking of Type 304 Austenitic Stainless Steel Under $MgCl_2$ and $FeCl_3$:$MgCl_2$ Droplets, *Corrosion*, 75, 2, (2018), 167-182 https://doi.org/10.5006/3026

[23] Takumi Haruna, Yang Wang, Jun Yamanishi, Hydrogen Absorption into Fe Plates with Rust Layers Containing Various $MgCl_2$ Amounts during Atmospheric Corrosion with Controlled Humidity, *ISIJ International*, 61, 4, (2021), 1179-1185 https://doi.org/10.2355/isijinternational.ISIJINT-2020-502

[24] Jayendra Srinivasan, Alana Margaret Parey, G. A. Marino, Tim Weirich, R. M. Asmussen, Rebecca Schaller, Eric Schindelholz, Jenifer Locke, Atmospheric Corrosion and Cracking of 304

Stainless Steel in Controlled Marine Atmospheres, *NACE Corrosion 2020*, United States, 2019

[25] Nor Roslina Rosli, Srdjan Nesic, Yoon-Seok Choi, David Young, Corrosion of UNS G10180 Steel in Supercritical and Subcritical CO_2 with O_2 as a Contaminant, *Nace Corrosion*, 2016

[26] Norhazilan Md Noor, Nordin Yahaya, Arman Abdullah, Mahmood Md Tahir, Lim Kar Sing, Microbiologically Influenced Corrosion of X-70 Carbon Steel by Desulfovibrio Vulgaris, *Advanced Science Letters*, 13, 1, (2012), 312-316 https://doi.org/10.1166/asl.2012.3768

[27] Xuehui Liu, Yongqiang Sui, Jianyuan Zhou, Yapeng Liu, Xiangbo Li, Jian Hou, Influence of available chlorine on corrosion behaviour of low alloy marine steel in natural seawater, *Corrosion Engineering, Science and Technology*, 58, 5, (2023), 475-481 https://doi.org/10.1080/1478422X.2023.2209961

[28] I. Saefuloh, N. Kanani, F. Gumelar Ramadhan, Y. Rukmayadi, Y. Yusuf, Syarif Abdullah, Sidik Susilo, The Study of Corrosion Behavior and Hardness of AISI SS 304 in Concentration of Chloride Acid Solution and Temperature Variations, *Journal of Physics: Conference Series*, 1477, 5, (2020), 052058 https://doi.org/10.1088/1742-6596/1477/5/052058

[29] Gadang Priyotomo, Lutviasari Nuraini, Siska Prifiharni, Sundjono Sundjono, Corrosion Behavior of Mild Steel in Seawater from Karangsong & Eretan of West Java Region, Indonesia, *Jurnal Kelautan: Indonesian Journal of Marine Science Technology*, 11, 2, (2018), 184-191 https://doi.org/10.21107/jk.v11i2.4335

[30] Shu Haibin, Song Yilin, Liu Junzhe, Effect of concentration difference of chloride ions on the corrosion of steel bar, *Proceedings of the 2018 7th International Conference on Energy, Environment and Sustainable Development (ICEESD 2018)*, 2018 https://doi.org/10.2991/iceesd-18.2018.160